COMPUTED- VERSUS ACQUIRED-DIFFUSION WEIGHTED IMAGING: A COMPARATIVE ANALYSIS OF PROSTATE CANCER DETECTION

N Hayat[1], J Mo[2], W H K Chiu[2]

1. Department of Diagnostic and Interventional Radiology, Kwong Wah Hospital, Hong Kong
2. Department of Diagnostic and Interventional Radiology, Queen Elizabeth Hospital, Hong Kong

INTRODUCTION

- Diffusion weighted imaging (DWI) is a core component of prostate multiparametric MRI for prostate cancer (PCa) detection as outlined in PI-RADS v2.1 [1].
- High *b*-value DWI (b >1,400s/mm^2) are used for its greater tumour conspicuity and detection, even for small lesions, compared to low or intermediate *b*-value (b 0-1,000 s/mm^2) DWI.
- Two accepted methods of acquiring high *b*-value DWI images are[1]:
  - **Acquired (aDWI):** direct acquisition
  - **Computed DWI (cDWI):** using mathematical models to synthesise high *b*-value images from a set of acquired lower *b*-value images.

aDWI high *b*-value	cDWI high *b*-value
• Requires additional imaging time (5 minutes) • Low signal-to-noise (SNR) • Increased susceptibility to distortion and artefacts	• No additional imaging time required • Higher SNR (better image quality) • No recognised standardisation on algorithm to compute cDWI images. • Image appearance can vary between different MRI vendors and software

- Although high *b*-value cDWI is accepted by the PI-RADS committee as part of its v2.1 guidelines[1], only several studies to date have directly compared the performance of cDWI and aDWI. These studies have mainly focused on DWI image analysis alone[2-5].

OBJECTIVE

"To assess and compare the diagnostic performance of high b-value cDWI and aDWI in the detection of PCa and to evaluate their effect on PI-RADS scoring."

MATERIALS & METHOD

PATIENT COHORT

- Retrospective, single-centre study.
- A search of the radiology information system at our institution, Queen Elizabeth Hospital, identified 619 consecutive MRI prostate exams performed between July 2020 and June 2024.
- **100 patients** with **329 biopsy-positive sites** were included.

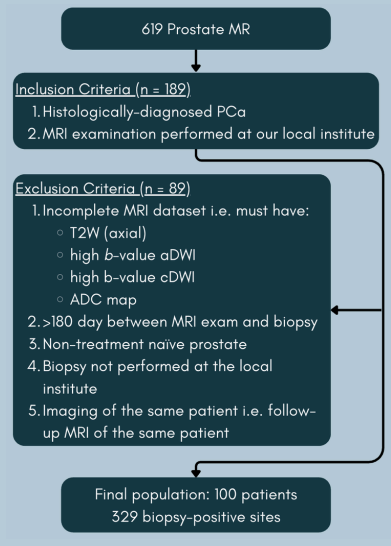

IMAGE ACQUISITION

- MRI exams were performed using a 3T MR scanner (MAGNETOM Skyra, Siemens Healthineers, Erlangen, Germany
- cDWI images for *b*-value 1,500 (cDWI$_{b1500}$) were generated to match the aDWI *b*1,500 (aDWI$_{b1500}$) acquired in accordance with our institutional protocol.
- cDWI$_{b1500}$ images were extrapolated based on a mono-exponential diffusion decay model, derived from low (*b*50) and intermediate (*b*500/800) *b*-value DWI acquisition.

PARAMETER	VALUE [median (Q1 - Q3)]
No. of patients	100 patients with 329 biopsy-positive sites
Age	71 (67 - 74)
Time from MRI to biopsy (days)	103 (47 - 145)
PSA (ng/mL)	8.1 (5.6 - 13.1)
Prostate volume (mL)	55.2 (37.5 - 68.5)
PSA density (ng/mL^2)	0.16 (0.11 - 0.30)

*Table 1. Patient demographic and characteristics.

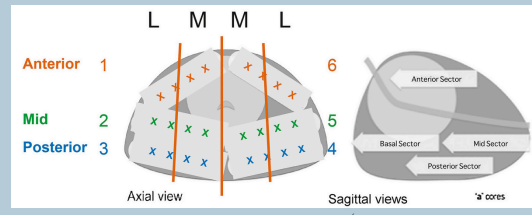

*Figure 1. Ginsburg biopsy protocol template 12 sector map[6]

MATERIALS & METHOD

IMAGE ANALYSIS

- Two board-certified radiologists independently reviewed $aDWI_{b1500}$ and $cDWI_{b1500}$ images of the 100 patients.
- Complete prostate MRI sequences including T2W and ADC map were provided.
- For each patient, the location of biopsy-positive sites were specified on a spreadsheet. Patient demographics and GS were withheld.
- A Ginsburg biopsy protocol sector map was provided as reference for correlating the biopsy-sites and MRI location.
- A DWI score of 1 to 5 was assigned to each biopsy-positive site for the $aDWI_{b1500}$ and $cDWI_{b1500}$ in accordance with PI-RADS scoring.
- A third independent radiologist assigned the T2W and ADC score for all 329 biopsy-positive sites. These scores were subsequently used to calculate a final PI-RADS score.

REFERENCE STANDARD

- **Biopsy:** Urologists at our local institution employ a modified Ginsburg systematic biopsy template using 12/14 sector approach[6].
- **Histopathology:** Conducted in accordance with ISUP (International Society of Urological Pathology) grading system[7]:
  - Clinically significant PCa (csPCa) was defined as Gleason Score (GS) of $\geqslant 7$.
  - Non-clinically significant PCa (non-csPCa) was defined as GS of 6.

CASE EXAMPLES

CASE 1

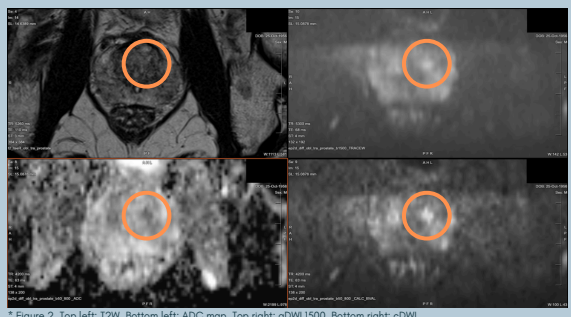

* Figure 2. Top left: T2W. Bottom left: ADC map. Top right: aDWI 1500. Bottom right: cDWI.

Pathology:
- GS 6 at left middle medial sector
- TZ lesion.

MRI Findings:
- aDWI score: 3, cDWI score: 4
- Score Diff c-aDWI = 1
- T2W score: 3, ADC score: 3

A difference in DWI score did not affect the final PI-RADS score, as upgrading a PI-RADS 3 lesion to 4 requires a combined DWI/ADC score of 4.

CASE 2

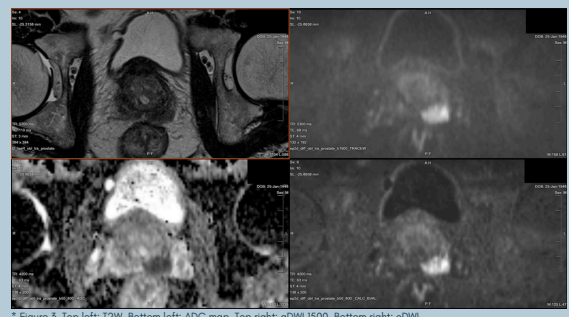

* Figure 3. Top left: T2W. Bottom left: ADC map. Top right: aDWI 1500. Bottom right: cDWI.

Pathology:
- GS 8 at left posterior medial + lateral sector.
- PZ lesion.

MRI Findings:
- Both observers awarded DWI score of 5 (1.7cm focal marked hyperintensity) for both aDWI and cDWI images.
- Score Diff c-aDWI = 0

No effect on PI-RADS score

RESULTS

PATIENT COHORT

- 329 biopsy-positive sites - distribution by:
  - **Location**: PZ (n=147), TZ (n=183).
  - **GS**: 6 (n=147), 7 (n=108), 8 (n=42), 9 (n=18), 10 (n=14).

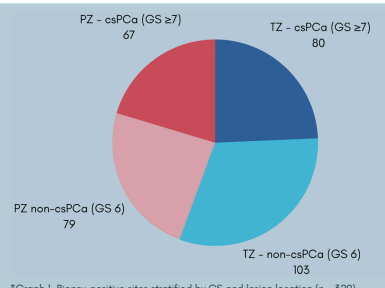

*Graph 1. Biopsy-positive sites stratified by GS and lesion location (n = 329).

RESULTS

INTEROBSERVER AGREEMENT

QUADRATIC-WEIGHTED KAPPA	cDWI b1500	aDWI b1500
ALL LESION	0.654 (95% CI, 0.582 to 0.718)	0.718 (95% CI, 0.655 to 0.771)
TZ	0.677 (95% CI, 0.580 to 0.756)	0.722 (95% CI, 0.635 to 0.794)
PZ	0.619 (95% CI, 0.501 to 0.716)	0.711 (95% CI, 0.615 to 0.792)

*Table 3. Interobserver agreement using Quadratic-weighted Kappa for overall and location subgroup.

- Interobserver agreement between the two DWI methods is substantial for all lesions and across location subgroups.
- Agreement is slightly lower for $cDWI_{b1500}$ across all groups.

COMPARISON OF cDWI and aDWI

- The mean DWI scores for both aDWI and cDWI are highly similar, indicating minimal systematic bias at the group level.

	cDWI b1500	aDWI b1500
DWI SCORE mean ± SD (95% CI)	2.94 ± 1.20 [2.808, 3.068]	2.91 ± 1.23 [2.777, 3.044]

*Table 4. DWI score mean for the cDWI and aDWI.

- The mean DWI scores for both aDWI and cDWI are highly similar, indicating minimal systematic bias at the group level.
- The mean observer difference in DWI score between $cDWI_{b1500}$ and $aDWI_{b1500a}$ was +0.03 [paired t-test: t = 0.88, p = 0.377 / Wilcoxon signed-rank test: W = 5012.5, p = 0.394]. Findings indicate no statistical significant difference seen between cDWI and aDWI scores.

- Subgroup analysis - by:
  - **Location:**
    - TZ (n = 183): mean paired difference = +0.00; W=1495.5, p=0.975.
      - No significant difference.
    - PZ (n = 146): mean paired difference = +0.06; W=1030.0, p=0.200.
      - No significant difference.
  - **GS:**
    - csPCa (n=182): mean paired difference = -0.03; W=1151.0, p=0.343
      - No significant difference.
    - non-CSPCa (n=147): mean paired difference = +0.10; W=1045.5, p=0.039
      - Small but statistically significant upward shift of c-DWI of non-cs PCa.

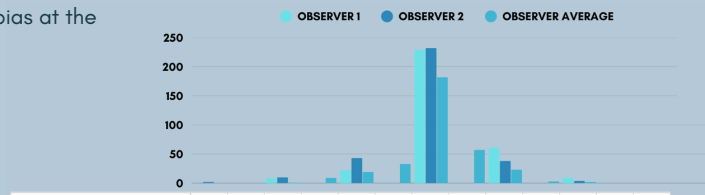

SCORE DIFF c-aDWI	-3	-2.5	-2	-1.5	-1	-0.5	0	0.5	1	1.5	2	2.5	3	Mean
OBSERVER 1 (n = 329)	0		8		22		229		61		9		0	
OBSERVER 2 (n = 329)	2		10		43		232		38		4		0	
OBSERVER-MEAN	0	0	1	9	19	33	182	57	23	3	2	0	0	

*Table 5 & Graph 2. DWI score differences calculated by subtracting $aDWI_{b1500}$ from $cDWI_{b1500}$ for all biopsy-positive sites (n = 329).

EFFECT ON PI-RADS SCORE

- The no. of lesions with a difference between their cDWI and aDWI scores was 147.
- After applying the DWI score change to the T2W and ADC scores, **18** of the **147 lesions** had a change in their PI-RADS score:
  - All in the PZ:
    - 9 in the csPCa group.
    - 9 in the non-CSPCa group.

	UP-SCORED		DOWN-SCORED	
csPCa	n = 1	PIRADS 3 > 4 (n = 1)	n = 7	PIRADS 3 > 2 (n = 2) PIRADS 4 > 3 (n = 5)
non-csPCa	n = 8	PIRADS 2 > 3 (n = 7) PIRADS 3 > 4 (n = 1)	n = 2	PIRDAS 4 > 3 (n = 1) PIRDAS 3 > 2 (n = 1)

CONCLUSION & LIMITATIONS

- **Conclusion:**
  - $cDWI_{b1500}$ and $aDWI_{b1500}$ demonstrate comparable diagnostic performance for PCa detection. A small but statistically significant upward shift in cDWI scores was observed in non-cs PCa.
- **Limitations:**
  - Localising MRI lesions using a biopsy sector map is inherently difficult. Furthermore, biopsy cores are obtained in a craniocaudal fashion whereas DWI/ADC images are typically interpreted in the axial plane.
  - Potential bias:
    - Detection bias - aDWI and cDWI images were explicitly labelled.
    - Confirmation bias - all cases have histology-confirmed PCa, which may subconsciously influenced DWI scoring.

REFERENCES:

1. Turkbey, B., Rosenkrantz, A. B., Haider, M. A., Padhani, A. R., Villeirs, G., Macura, K. J., Tempany, C. M., Choyke, P. L., Cornud, F., Margolis, D. J., Thoeny, H. C., Verma, S., Barentsz, J., & Weinreb, J. C. (2019). Prostate Imaging Reporting and Data System Version 2.1: 2019 Update of Prostate Imaging Reporting and Data System Version 2. European Urology, 76(5), 540-551. https://doi.org/10.1016/j.eururo.2019.02.033
2. Jensoubi, S., Wagner, M., Montagne, S., Ezziane, M., Mespoulet, J., Comperat, E., Estellat, C., Baptiste, A., & Renard-Penna, R. (2019). MRI for prostate cancer: can computed high b-value DWI replace native acquisitions? European Radiology, 29(10), 5197-5204. https://doi.org/10.1007/s00330-019-06085-z
3. Ueno, Y. R., Tamada, T., Takahashi, S., Tanaka, U., Sofue, K., Kanda, T., Nogami, M., Ohno, Y., Hinata, N., Fujisawa, M., & Murakami, T. (2018). Computed Diffusion-Weighted Imaging in Prostate Cancer: Basics, advantages, cautions, and future prospects. Korean Journal of Radiology, 19(5), 852. https://doi.org/10.3348/kjr.2018.19.5.852
4. Kallis, K., Conlin, C. C., Zhong, A. Y., Hussain, T. S., Chatterjee, A., Karczmar, G. S., Rakow-Penner, R., Dale, A. M., & Seibert, T. M. (2024). Comparison of synthesized and acquired high b-value diffusion-weighted MRI for detection of prostate cancer. Cancer Imaging, 24(1). https://doi.org/10.1186/s40644-024-00725-6
5. Kim, Y. J., Kim, S. H., Baek, T. W., Park, H., Lim, Y., Jung, H. K., & Kim, J. Y. (2022). Comparison of Computed Diffusion-Weighted Imaging b2000 and Acquired Diffusion-Weighted Imaging b2000 for Detection of Prostate Cancer. Journal of the Korean Society of Radiology, 83(5), 1059. https://doi.org/10.3348/jksr.2022.0004
6. Hansen, N., Patruno, G., Wadhwa, K., Gaziev, G., Miano, R., Barrett, T., Gnanapragasam, V., Doble, A., Warren, A., Bratt, O., & Kastner, C. (2016). Magnetic resonance and ultrasound image fusion supported transperineal prostate biopsy using the Ginsburg Protocol: technique, learning points, and biopsy results. European Urology, 70(2), 332-340. https://doi.org/10.1016/j.eururo.2016.02.064
7. Van Leenders, G. J., Van Der Kwast, T. H., Grignon, D. J., Evans, A. J., Kristiansen, G., Kweldam, C. F., Litjens, G., McKenney, J. K., Melamed, J., Mottet, N., Paner, G. P., Samaratunga, H., Schoots, I. G., Simko, J. P., Tsuzuki, T., Varma, M., Warren, A. Y., Wheeler, T. M., Williamson, S. R., & Iczkowski, K. A. (2020). The 2019 International Society of Urological Pathology (ISUP) Consensus Conference on Grading of Prostatic Carcinoma. The American Journal of Surgical Pathology, 44(8), e87-e99. https://doi.org/10.1097/pas.0000000000001497